

Metastability and anomalous fixation in evolutionary games on scale-free networks

Michael Assaf^{*1} and Mauro Mobilia^{*2}

¹*Loomis Laboratory of Physics, Department of Physics 1110 West Green Street, Urbana, Illinois 61801, U.S.A*

²*Department of Applied Mathematics, School of Mathematics, University of Leeds, Leeds LS2 9JT, U.K.*

We study the influence of complex spatial structure on the metastability and fixation properties of a set of evolutionary processes characterized by frequency-dependent selection. In the framework of evolutionary game theory, we analyze the dynamics of snowdrift games (characterized by a metastable coexistence state) on scale-free networks. Using an effective diffusion theory we demonstrate how the complex structure of the network affects the system's metastable state and leads to *anomalous fixation*. In particular, we analytically and numerically show that the probability and mean time of fixation are characterized by stretched exponential behaviors with exponents depending nontrivially on the network's degree distribution. Our approach is also shown to be applicable to models, like coordination games, characterized by the *absence* of metastability prior to fixation.

PACS numbers: 05.40.-a, 02.50.Ey, 87.23.Kg, 64.60.aq

The dynamics of systems where successful traits spread at the expense of others is naturally modeled in the framework of evolutionary game theory (EGT) [1]. EGT involves frequency-dependent selection, where selection depends on the species instantaneous concentration. Traditionally EGT is studied in terms of differential equations, and is an approach transcending almost every aspect of evolutionary biology [1, 2]. While the EGT classic setting was originally proposed to describe the evolution of infinitely large and spatially homogeneous populations, it is known that evolutionary dynamics is affected by demographic noise and by the population's spatial arrangement (structure) [3–5]. Evolutionary dynamics is often characterized by the central notion of fixation, first introduced in population genetics [6], that refers to the possibility that a “mutant type” takes over the entire population. In contrast to spatially-homogeneous (well-mixed) populations, accounting for the population's spatial arrangement can give rise to various scenarios: *e.g.*, in games modeling social dilemmas, the local interactions on regular lattices may enhance or inhibit the resistance of “cooperators” against the invasion by “defectors” [4]. In this context, evolutionary dynamics on networks [7] provides a general and unifying framework to describe the dynamics of both well-mixed and spatially-structured populations [8]. In spite of their importance, fixation of evolutionary processes on networks have been mostly studied in idealized situations, *e.g.* for two-state systems under a constant weak selective bias [8–11]. In these works, it has been shown that the update rules and the network structure effectively renormalize the population size and affect the fixation properties. While these results are of great interest, they do not account for *frequency-dependent selection*, which is an important evolutionary mechanism [1, 6], and may lead to a long-lived *metastable*

(or coexistence) state prior to fixation [12, 13]. As a firm understanding of metastability on complex networks is still lacking, we here study metastability and fixation on a class of scale-free networks in the EGT framework. Our findings will also be directly relevant to the dynamics of epidemic outbreaks [14] and population genetics [15].

Here, we study “snowdrift games” (SGs, see below) [1, 13] that are the paradigmatic EGT models exhibiting metastability (see [16] for their experimental relevance). In the case of well-mixed populations (complete graphs), the fixation properties of SGs typically exhibit an exponential dependence on the population size, see *e.g.* [13]. Using an individual-based approach, we show that the spatial structure of scale-free networks yields *anomalous* fixation and metastability characterized by a stretched exponential dependence on the population size, in stark contrast with their non-spatial counterparts. We also show that such a dependence characterizes fixation in models like coordination games which do *not* possess a long-lived metastable state prior to fixation [1].

The model. We consider a network comprising N nodes, each of which is either occupied by an individual of type C (cooperator) or by a D-individual (defector). The occupancy of the node i is encoded by the random variable η_i , with $\eta_i = 1$ if the node i is occupied by a C and $\eta_i = 0$ otherwise. The state of the system is thus described by $\{\boldsymbol{\eta}\} = \{\eta_i\}^N$ and the density of cooperators present in the system is $\rho \equiv \sum_{i=1}^N \eta_i / N$. The network is specified by its adjacency matrix $\mathbf{A} = [A_{ij}]$, whose elements are 1 if the nodes ij are connected and 0 otherwise. The network is also characterized by its degree distribution $n_k = N_k / N$, where N_k is the number of nodes of degree k . EGT is traditionally concerned with large and homogeneous populations (i.e. $N \rightarrow \infty$ and $A_{ij} = 1, \forall ij$) whose mean field dynamics is described by the celebrated replicator equation [1, 2]: $(d/dt)\rho(t) = \rho(t)(1 - \rho(t))[\Pi^C(\rho) - \Pi^D(\rho)]$, where $\Pi^{C/D}(\rho)$ are the cooperator/defector average payoffs derived from the game's payoff matrix. For a generic two-strategy cooper-

^{*}The authors contributed equally to this work.

ation dilemma, the payoff of C against another C is denoted a and that of D playing against D is d . When C and D play against each other, the former gets payoff b and the latter gets c [1]. Here, we are particularly interested in SGs, for which $c > a$ and $b > d$. SGs are characterized by a stable interior fixed point $\rho_* = (d-b)/(a-b-c+d)$ and unstable absorbing states $\rho = 0$ (all-D) and $\rho = 1$ (all-C). When the population size is finite ($N < \infty$), the role of fluctuations is important and ρ_* becomes a *metastable* state whose decay time on complete graphs ($A_{ij} = 1, \forall ij$) grows exponentially with N [13].

In a spatial setting, the interactions are among nearest-neighbor individuals and the species payoffs are defined locally: C and D players at node i interacting with a neighbor at site j respectively receive payoffs $\Pi_{ij}^C = a\eta_j + b(1-\eta_j)$ and $\Pi_{ij}^D = c\eta_j + d(1-\eta_j)$. In the spirit of the Moran model (in the weak selection limit) [2, 5, 6], each species local reproductive potential, or fitness, is given by the difference of $\Pi_{ij}^{C/D}$ relative to the population mean payoff $\bar{\Pi}_{ij}(t)$. Here, we make the mean-field-like choice $\bar{\Pi}_{ij}(t) = \rho(t)\Pi_{ij}^C + (1-\rho(t))\Pi_{ij}^D$ to include what arguably is the simplest mechanism ensuring the formation of metastability. It is customary to introduce a selection strength s in the definition of the fitness to unravel the interplay between random fluctuations and selection [2, 5, 6]. Here, the fitnesses of C/D at node i interacting with a neighbor at site j are

$$f_{ij}^C = 1 + s[\Pi_{ij}^C - \bar{\Pi}_{ij}] \quad \text{and} \quad f_{ij}^D = 1 + s[\Pi_{ij}^D - \bar{\Pi}_{ij}]. \quad (1)$$

These expressions comprise a baseline contribution (set to 1) and a selection term proportional to the relative payoffs. Moreover, we consider a system evolving according to the so-called “link dynamics” (LD) [9, 10]: a link is randomly selected at each time step and if it connects a CD pair, one of the neighbors is randomly selected for reproduction with a rate proportional to its fitness while the other is replaced by the offspring [17]. Fixation under LD is unaffected by the network topology when the selection is frequency-independent [10]. However, in the more generic case of frequency-dependent selection considered here, metastability and fixation properties are drastically altered by the network’s structure, as shown below.

The evolutionary dynamics of the system will be analyzed in terms of the (subgraph) density $\rho_k = \sum_i \eta_i / N_k$ of cooperators C on nodes of degree k (the prime means that the sum is restricted to nodes of degree k). Quantities necessary for our analysis are the m^{th} -moment of the degree distribution, $\mu_m \equiv \sum_k k^m n_k = \sum_i k_i^m / N$, where k_i denotes the degree of node i , and the degree-weighted density of cooperators $\omega \equiv \sum_k (k/\mu_1) n_k \rho_k$.

Effective diffusion theory. To implement the evolutionary dynamics, we introduce $\Psi_{ij} = \eta_i(1-\eta_j)f_{ij}^C$ and $\Psi_{ji} = (1-\eta_i)\eta_j f_{ij}^D$, where $\eta_i(1-\eta_j)$ is non-zero only when the nodes ij are occupied by a CD pair. In the LD, the probability to select the neighbor j of node i for an

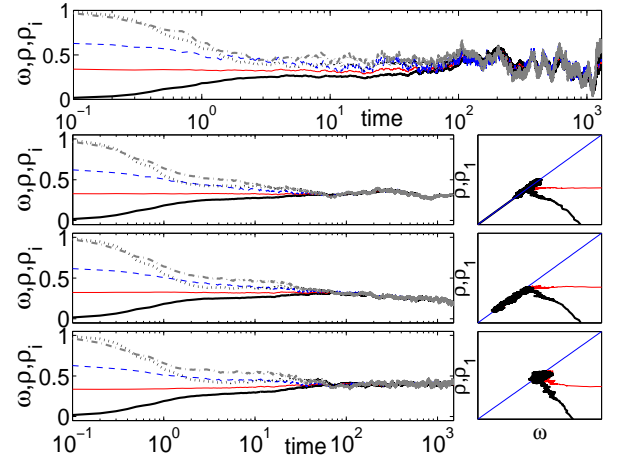


FIG. 1: (Color online). Densities ρ (thin solid), ω (dashed), ρ_1 (thick solid), ρ_2 (dotted), ρ_3 (dashed-dotted), on a scale-free network with $\nu = 3$ for a SG with $a = d = 1, b = 1.4, c = 1.6$. Initially $\rho_{k>\mu_1}(0) = 1, \rho_{k\leq\mu_1}(0) = 0$. Top panel: Single realization for $s = 0.001$ and $N = 10^4$. Left/right lower panels: Trajectories averaged over 500 samples ($N = 2000$) for $s = 0.001$ (top), $s = 0.01$ (middle), $s = 0.1$ (bottom). Right: ρ and ρ_1 versus ω (the straight line is an eye guide).

update is $A_{ij}/(N\mu_1)$ and the transition $\eta_i \rightarrow 1-\eta_i$ hence occurs with probability $\sum_j \frac{A_{ij}}{N\mu_1} [\Psi_{ij} + \Psi_{ji}]$ [10]. The subgraph density ρ_k changes by $\pm\delta\rho_k = \pm 1/N_k$ according to a birth-death process [18] defined by the transition rates $T^+(\rho_k) = \sum_i \sum_j A_{ij} \Psi_{ji} / (N\mu_1)$ and $T^-(\rho_k) = \sum_i \sum_j A_{ij} \Psi_{ij} / (N\mu_1)$, respectively. For our analytical treatment, we focused on degree-heterogeneous networks with degree-uncorrelated nodes, as in Molloy-Reed networks (MRN) [19], yielding $A_{ij} = k_i k_j / (N\mu_1)$. Our numerical simulations were performed using the “redirection algorithm” that generates degree-correlated scale-free networks [20]. Yet, it has been shown that the dynamics of the latter is close to that on MRN [10]. With $\sum_i N^{-1} = n_k \rho_k$, the transition rates become

$$T^+(\rho_k) \equiv T_k^+ = (n_k/\mu_1) [1 + s(b-d)(1-\rho)] k(1-\rho_k)\omega \\ T^-(\rho_k) \equiv T_k^- = (n_k/\mu_1) [1 - s(a-c)\rho] k\rho_k(1-\omega). \quad (2)$$

We notice that T_k^\pm are nonzero provided that the mean degree μ_1 does not diverge with $N \rightarrow \infty$ [21]. In the limit of weak selection intensity ($s \ll 1$) [13], one can use the diffusion theory to treat the birth-death process defined by (2). This yields a multivariate backward Fokker-Planck equation (FPE) whose generator reads

$$\mathcal{G}(\{\rho_k\}) = \sum_k \left[\frac{(T_k^+ - T_k^-)}{n_k} \frac{\partial}{\partial \rho_k} + \frac{(T_k^+ + T_k^-)}{2Nn_k^2} \frac{\partial^2}{\partial \rho_k^2} \right], \quad (3)$$

with time increments $\delta t = N^{-1}$ [6, 18]. Moreover, when the selection intensity is weak ($s \ll 1$), a timescale separation allows to greatly simplify the

analysis [10, 11]. Indeed, when $t \ll s^{-1}$ the selection pressure is negligible and the quantity ρ is conserved [9]. In fact, using (2) at mean field level gives $(d/dt)\bar{\rho} = s(a - b - c + d)\bar{\omega}(1 - \bar{\omega})(\bar{\rho} - \rho_*)$ (where the upper bar denotes the ensemble average). This indicates that $\bar{\rho}$ relaxes to its metastable value ρ_* on a timescale $t \sim s^{-1} \gg 1$, see Fig. 1. At mean field level, Eqs. (2) also yields $(d/dt)\bar{\rho}_k = (T_k^+(\bar{\rho}_k) - T_k^-(\bar{\rho}_k))/n_k = (k/\mu_1) \times \{\bar{\omega} - \bar{\rho}_k + s[(b-d)\bar{\omega}(1-\bar{\rho})(1-\bar{\rho}_k) + (a-c)(1-\bar{\omega})\bar{\rho}_k\bar{\rho}]\}$. This indicates that after a timescale of order $\mathcal{O}(1)$, $\bar{\rho}_k \approx \bar{\omega}$, and also $\bar{\rho} \approx \bar{\omega}$ since $\bar{\rho} = \sum_k \bar{\rho}_k n_k$. With $\bar{\rho}_k \approx \bar{\omega} \approx \bar{\rho}$, the rate equation for $\bar{\rho}_k$ becomes $(d/dt)\bar{\rho}_k \simeq -(k/\mu_1)(b-d)s(1-\bar{\rho}_k)\bar{\rho}_k(\bar{\rho}_k/\rho_* - 1)$. Hence, while after a time of order $\mathcal{O}(1)$, $\bar{\rho}_k \approx \bar{\omega} \approx \bar{\rho}$, all these quantities approach ρ_* on a longer timescale $t \sim s^{-1}$. This behavior is corroborated by numerical simulations, see Fig. 1 [22]. Because fixation occurs on much longer time-scales than s^{-1} (see below), we henceforth use the approximation that on average $\rho_k \approx \rho \approx \omega$. Using Eq. (3), changing variables $\rho_k \rightarrow \omega$ and using the definition of ω that yields $\partial_{\rho_k} \rightarrow (kn_k/\mu_1)\partial_\omega$, we arrive at the *effective single-coordinate* FPE generator [10, 11]

$$\mathcal{G}_{\text{eff}}(\omega) = \frac{\omega(1-\omega)}{N_{\text{eff}}} \left[-\sigma(\omega - \rho_*) \frac{\partial}{\partial \omega} + \frac{1}{2} \frac{\partial^2}{\partial \omega^2} \right]. \quad (4)$$

Here $\sigma \equiv 2(b-d)N_{\text{eff}}s_{\text{eff}}/\rho_*$, and the effective population size and selection intensity are given by $N_{\text{eff}} \equiv N(\mu_1)^3/\mu_3$ and $s_{\text{eff}} \equiv s\mu_2/(\mu_1)^2$. For scale-free networks with degree distribution $n_k \propto k^{-\nu}$ and finite average degree (i.e. $\gamma > 2$) [21], the maximum degree is $k_{\text{max}} \sim N^{1/(\nu-1)}$ [23]. This can be used to calculate the moments μ_m [10] and obtain the scaling of $N_{\text{eff}}s_{\text{eff}}$:

$$\sigma = \frac{2(b-d)}{\rho_*} sN \frac{\mu_1\mu_2}{\mu_3} \sim \begin{cases} sN, & \nu > 4 \\ sN/\ln N, & \nu = 4 \\ sN^{(2\nu-5)/(\nu-1)}, & 3 < \nu < 4 \\ s\sqrt{N} \ln N, & \nu = 3 \\ sN^{(\nu-2)/(\nu-1)}, & 2 < \nu < 3. \end{cases} \quad (5)$$

We have checked analytically and by numerical simulations that our theory is valid when $s_{\text{eff}}^2 \ll N_{\text{eff}}^{-1}$. Hence, for $2 < \nu < 4$ it is applicable over a broader range of values of s than on complete graphs; e.g. $s^2 \ll N^{-1/(\nu-1)}$ when $2 < \nu < 3$ ($s^2 \ll N^{-1}$ on complete graphs [13]).

Fixation properties. Evolutionary dynamics is characterized by the fixation probability $\phi^C(\omega)$ that a system with initial degree-weighted density ω is taken over by cooperators. In the framework of the effective diffusion theory and using (4) the fixation probability obeys $\mathcal{G}_{\text{eff}}(\omega)\phi^C(\omega) = 0$ with the boundary conditions $\phi^C(0) = 1 - \phi^C(1) = 0$ [5, 18]. The solution of this equation is

$$\phi^C(\omega) = \frac{\text{erfi}[\rho_*\sqrt{\sigma}] - \text{erfi}[(\rho_* - \omega)\sqrt{\sigma}]}{\text{erfi}[\rho_*\sqrt{\sigma}] + \text{erfi}[(1 - \rho_*)\sqrt{\sigma}]}, \quad (6)$$

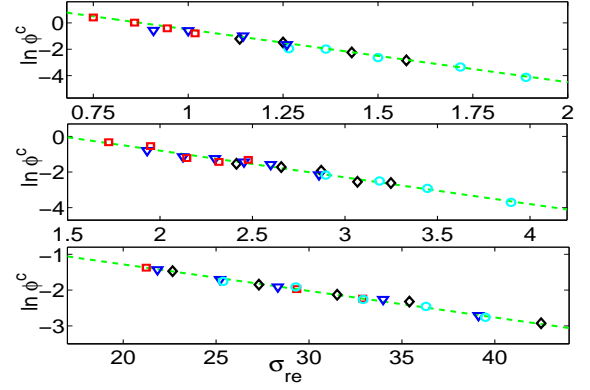


FIG. 2: (Color online). Fixation probability ϕ^C versus rescaled $\sigma_{\text{re}} \propto \sigma$ [see (5)] for SGs with $a = d = 1$, $b = 1.05$, $c = 1.075$ ($\rho_* = 0.4$) and $s = 0.075$ (\square), 0.1 (\triangle), 0.125 (\diamond) and 0.15 (\circ). Numerical results for $\nu = 2.5$ (top), $\nu = 2.75$ (middle), $\nu = 3$ (bottom) collapse linearly (dashed) with $-sN\mu_1\mu_2/\mu_3$, in agreement with the theory, see text. Here $N = 1000 - 4000$ and initially $\rho_k = \rho = \omega = 100/N$.

where $\text{erfi}(z) \equiv \frac{2}{\sqrt{\pi}} \int_0^z e^{u^2} du$. Let us consider the (biologically relevant) case of a small initial density of cooperators such that $\omega \ll 1$, weak selection [5, 6], and a large population such that $\rho_*^2\sigma \gg 1$ and metastability is guaranteed. Using the asymptote $\text{erfi}(x) \sim e^{x^2}$ for $x \gg 1$ in Eq. (6), we distinguish two cases: (i) when $\rho_* < 1/2$, $\ln \phi^C \simeq -(1 - 2\rho_*)\sigma$; (ii) when $\rho_* > 1/2$ and $\omega > 2\rho_* - 1$, $\ln(1 - \phi^C) \simeq -(2\rho_* - 1)\sigma$, while $\ln(1 - \phi^C) \simeq -\omega(2\rho_* - \omega)\sigma$ if $\rho_* > 1/2$ and $\omega < 2\rho_* - 1$. The stretched-exponential dependence of ϕ^C on N is shown in Fig. 2 where (as in Figs. 3 and 4) data have been rescaled and collapsed with $\sigma \propto sN\mu_1\mu_2/\mu_3$ along a single line. Since $\ln \phi^C \sim -N$ on complete graphs [13], our results demonstrate how the complex structure of the network drastically affects the fixation probability.

Another quantity of great interest is the (unconditional) mean fixation time (MFT) $\tau(\omega)$ – the mean time necessary to reach an absorbing boundary. Here, using Eq. (4) the MFT is obtained by solving $\mathcal{G}_{\text{eff}}(\omega)\tau(\omega) = -1$ with the boundary conditions $\tau(0) = \tau(1) = 0$ [10, 11]. Using standard methods [6, 18], we obtain

$$\tau(\omega) = 2N_{\text{eff}} \left[(1 - \phi^C(\omega)) \int_0^\omega dy \frac{e^{-\Theta(y)}}{y(1-y)} \int_0^y dz e^{\Theta(z)} + \phi^C(\omega) \int_\omega^1 dy \frac{e^{-\Theta(y)}}{y(1-y)} \int_y^1 dz e^{\Theta(z)} \right]; \quad \Theta(z) \equiv \sigma z(z - 2\rho_*).$$

For $\rho_*^2\sigma \gg 1$ the inner integrals can be computed by expanding $\Theta(z)$ around its extremal values ($z = 0$ for $z \in [0, \rho_*]$ and $z = 1$ for $z \in [\rho_*, 1]$), while the outer integral is computed via the saddle-point approximation around $\omega = \rho_*$. To leading order, one thus obtains $\tau(\omega) \sim (1 - \phi^C(\omega))e^{\sigma\rho_*^2}$ when $\omega > \rho_*$ and $\tau(\omega) \sim \phi^C(\omega)e^{\sigma(1-\rho_*)^2}$ otherwise. When $\sigma \gg 1$ and $\rho_* < 1/2$ (as in Fig. 3), we

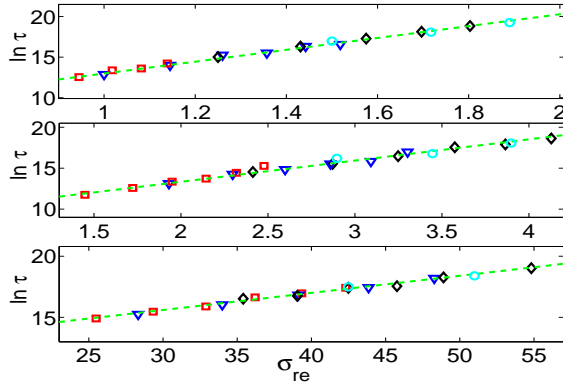


FIG. 3: (Color online). MFT τ versus rescaled $\sigma_{\text{re}} \propto \sigma$ for $\nu = 2.5$ (top), $\nu = 2.75$ (middle), and $\nu = 3$ (bottom). Numerical results (symbols) collapse along lines (dashed) in agreement with (7), see text. Here, symbols and parameters are the same as in Fig. 2, and initially $\rho_k = \rho = \omega = 0.5$.

find that $\tau(\omega)$ grows with N as a stretched exponential:

$$\ln \tau(\omega) \simeq \sigma \rho_*^2. \quad (7)$$

When the initial number of cooperators is not too low, the long-lived metastable state is entered prior to fixation and the MFT (7) is independent of the initial condition [12, 13]. Eq. (7), confirmed by Fig. 3, implies that for scale-free networks with $2 < \nu < 4$ fixation occurs much more rapidly than on complete graphs, a phenomenon called “hyperfixation” in population genetics [15].

For completeness, we have also studied the class of “coordination games” (CGs) characterized (at mean-field level) by an unstable interior (coexistence) fixed point and two stable absorbing states [1]. The fixation probability of CGs evolving under the LD on scale-free graphs has been found to have the same stretched-exponential dependence on N as in the SGs [13], see Fig. 4.

Discussion & conclusion. We have studied metastability and fixation of evolutionary processes on scale-free networks in the realm of EGT. Within an individual-based approach, we have focused on “snowdrift games” with frequency-dependent selection evolving according to the LD [10] and characterized by long-lived (metastable) coexistence. Exploiting a timescale separation occurring at weak selection intensity, we have devised an effective (single-coordinate) diffusion theory and, from the corresponding backward Fokker-Planck equation, calculated the probability and mean time of fixation. These quantities exhibit an stretched-exponential dependence on the population size, in stark contrast with their non-spatial counterparts. Here, important consequences of the stretched-exponential behaviors are a drastic reduction of the mean fixation time and the possible enhancement of the fixation probability of a few mutants with respect to a non-spatial setting. These anomalous fixation properties reflect the influence of the network’s complex

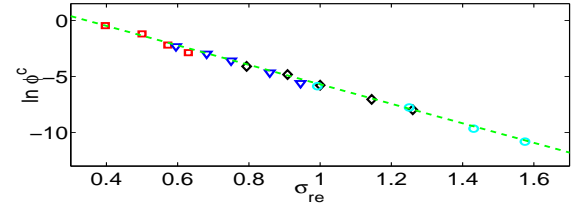


FIG. 4: (Color online). Fixation probability ϕ^C versus $\sigma_{\text{re}} \propto \sigma$ for CG with $\nu = 2.5$, $a = 1.6$, $b = c = 1$ and $d = 1.2$ ($\rho_* = 0.75$) and $s = 0.05$ (\square), 0.075 (\triangle), 0.1 (\diamond) and 0.125 (\circ). Numerics are consistent with the theoretical result $\ln \phi^C \sim -sN\mu_1\mu_2/\mu_3$. Here $N = 1000 - 4000$ and $\rho_k(0) = 0.5$.

structure on the evolutionary dynamics.

-
- [1] J. Maynard Smith, *Evolution and the Theory of Games* (Cambridge University Press, Cambridge, 1982); J. Hofbauer and K. Sigmund, *Evolutionary Games and Population Dynamics* (Cambridge University Press, Cambridge, 1998); G. Szabó and G. Fáth, Phys. Rep. **446**, 97 (2007).
 - [2] M. A. Nowak, *Evolutionary Dynamics* (Belknap Press, 2006).
 - [3] A. Traulsen *et al.*, Proc. Nat. Acad. Sci. USA **107**, 2962 (2010).
 - [4] M. A. Nowak and R. M. May, Nature **359**, 826 (1992); C. Hauert and M. Doebeli, Nature **428**, 643 (2004); M. Nowak, Science **314**, 1560 (2006).
 - [5] M. A. Nowak *et al.*, Nature **428**, 646 (2004); A. Traulsen *et al.*, Phys. Rev. E **74**, 021905 (2006).
 - [6] J. F. Crow and M. Kimura, *An Introduction to Population Genetics Theory* (Blackburn Press, New Jersey, 2009); W. J. Ewens, *Mathematical Population Genetics* (Springer, New York, 2004).
 - [7] A. L. Barabási and R. Albert, Science **286**, 509 (1999); R. Albert and A. L. Barabási, Rev. Mod. Phys. **74**, 47 (2002); M. E. J. Newman, SIAM Rev. **45**, 167 (2003).
 - [8] E. Lieberman *et al.*, Nature **433**, 312 (2005); H. Ohtsuki *et al.*, Nature **441**, 502 (2006).
 - [9] C. Castellano, D. Vilone, and A. Vespignani, EPL **63**, 153 (2003); K. Suchecki, V. M. Eguiluz, M. San Miguel, EPL **69**, 228 (2005).
 - [10] V. Sood and S. Redner, Phys. Rev. Lett. **94**, 178701 (2005); T. Antal *et al.*, Phys. Rev. Lett. **96**, 188104 (2006); V. Sood *et al.*, Phys. Rev. E **77**, 041121 (2008); G. J. Baxter, R. A. Blythe, and A. J. McKane, Phys. Rev. Lett. **101**, 258701 (2008); R. A. Blythe, J. Phys. A: Math. Theor. **43**, 385003 (2010).
 - [11] M. Assaf and B. Meerson, Phys. Rev. Lett. **97**, 200602 (2006); Phys. Rev. E **81**, 021116 (2010).
 - [12] M. Mobilia and M. Assaf, EPL **91**, 10002 (2010); M. Assaf and M. Mobilia, J. Stat. Mech., **P09009** (2010).
 - [13] R. Pastor-Satorras and A. Vespignani, Phys. Rev. Lett. **86**, 3200 (2001); R. M. May and A. L. Lloyd, Phys. Rev. E **64**, 066112 (2001); M. E. J. Newman, Phys. Rev. E **66**, 016128 (2002); R. Durrett, Proc. Nat. Acad. Sci. USA **107**, 4491 (2010).
 - [14] P. A. Wigham *et al.*, Th. Pop. Biol. **74**, 283 (2008).

- [16] J. Gore *et al.*, Nature **459**, 253 (2009).
- [17] The dynamics can also be implemented according to the voter model or the invasion process. While these and the LD are equivalent on degree-regular graphs, they are markedly different on degree-heterogeneous graphs [10].
- [18] C. W. Gardiner, *Handbook of Stochastic Methods*, (Springer, New York, 2002).
- [19] M. Molloy and B. Reed, Random. Struct. Algorithms **6**, 161 (1995).
- [20] S. N. Dorogovtsev, J. F. F. Mendes, and A. N. Samukhin, Phys. Rev. Lett. **85**, 4633 (2000); P. L. Krapivsky and S. Redner, Phys. Rev. E **63**, 066123 (2001).
- [21] Our model does not apply to (unrealistic) graphs with $\gamma \leq 2$, i.e. with diverging average degree μ_1 , see Eqs. (2).
- [22] This approximation deteriorates for increasing s [Fig. 1 (right)]. When $s = \mathcal{O}(1)$, generally $\bar{\rho}_k$ does not converge to $\bar{\omega}$. Moreover, the diffusion theory breaks down [13].
- [23] P. L. Krapivsky and S. Redner, J. Phys. A **35**, 9517 (2002).